A high-spin molecular wheel from self-assembled '*Mn rods*'†‡

Maria Manoli,[a] Alessandro Prescimone,[a] Abhudaya Mishra,[b] Simon Parsons,[a] George Christou[b] and Euan K. Brechin*[a]

Received 5th October 2006, Accepted 5th December 2006
First published as an Advance Article on the web 15th December 2006
DOI: 10.1039/b614492f

A Mn_{16} wheel-like molecule made from the self-assembly of Mn 'rods' in alcohol displays an $S = 14$ spin ground state and slow magnetisation relaxation consistent with single-molecule magnetism behaviour.

In recent years the synthesis of polymetallic clusters of Mn has largely been driven by the discovery of single-molecule magnetism.[1] Despite a wide range of transition metal clusters displaying slow magnetisation relaxation, the vast majority are complexes containing multiple Mn^{III} ions.[2] This stems from the 'unusually' large spin ground states often displayed by (primarily) mixed-valent Mn clusters in combination with the presence of Jahn–Teller distorted Mn^{III} ions, which provide the source of significant magnetoanisotropy.[3] Single-molecule magnets (SMMs) now range in nuclearity from two to eighty-four,[4] displaying a plethora of metal topologies, but rare amongst these are complexes derived from loop or wheel-like structures. Metal wheels are commonly encountered in Cr, Fe and V chemistry,[5] but examples in Mn chemistry remain surprisingly rare. Although a number of hexanuclear loops and metallocycles have been reported, larger examples are restricted to $[Mn^{III}_4Mn^{II}_4(O_2CCH_2{}^tBu)_{12}(teaH)_4]$,[6a] $[Mn^{III}(C_{14}H_9N_2O_3)(MeOH)]_{10}$,[6b] $[Mn^{III}_6Mn^{II}_6(O_2CMe)_{14}(mda)_8]$,[6c,d] $[Mn^{III}_8Mn^{II}_8(O_2CMe)_{16}(teaH)_{12}]$,[6a] and $[Mn^{III}_{84}O_{72}(OH)_6(OMe)_{24}(O_2CMe)_{78}(MeOH)_{12}(H_2O)_{42}]$.[4]

We have been exploring the reactivity of tripodal alcohol ligands in the synthesis of 3d transition metal SMMs.[7] When fully deprotonated, the disposition of the three alkoxide arms of the tri-anion generally directs the formation of triangular $[M_3]$ units where each arm of the ligand bridges one edge of the triangle. In the presence of co-ligands such as carboxylates or β-diketonates *etc*, these smaller units can combine in diverse ways to produce complexes whose structures range from 'simple' $[M_3]$ or $[M_4]$ (centred) triangles to "rod-like" complexes describing 'one dimensional' arrays of edge-sharing triangles; planar disc-like complexes describing 'two dimensional' arrays of edge-sharing triangles; and more complicated 'three dimensional' arrays commonly based on tetrahedra, octahedra and icosahedra.[7] Here we describe the synthesis, structure and magnetic properties of an unusual high-spin Mn_{16} loop constructed from two self-assembled planar Mn rods.

Reaction of $[Mn_3O(O_2CMe)_6(HIm)_3](O_2CMe)$ (0.58 mmol, 0.5 g) in MeOH (20 ml) with H_3tmp (0.58 mmol, 0.078 g) for 0.5 h results in the isolation of $[Mn_{16}O_2(OMe)_{12}(tmp)_8(O_2CMe)_{10}]\cdot 3Et_2O$ ($\mathbf{1}\cdot 3Et_2O$), which crystallized during 3 d of diffusion of diethyl ether into the filtered solution.

Complex **1** (Fig. 1) crystallises in the triclinic space group $P\bar{1}$.§ The core of the complex consists of a central near-planar $Mn^{III}{}_{10}$ single-stranded loop to which a further six Mn ions are attached—three above and three below opposite sides of the Mn_{10} plane (Mn1, Mn3, Mn5). The metallic skeleton (Fig. 1) thus describes two off-set parallel Mn_7 'rods' (comprising five edge-sharing triangles) linked by two apical Mn ions (Mn8 and symmetry equivalent) into a loop. A family of Mn rod-like molecules, including a heptametallic complex, with near identical structures (but differing oxidation levels) has been reported previously.[7] Each half of the $Mn_{16}O_{30}$ metal–oxygen core (Fig. 1) describes two Mn_3O_4 partial cubes (comprising Mn1, Mn2, Mn4 and Mn5, Mn6, Mn7) linked to a central Mn_3O triangle (Mn3, Mn4, Mn6) *via* the oxygen atoms of $\eta^1{:}\eta^1{:}\eta^2{:}\mu\text{-tmp}^{3-}$ and $\mu\text{-}O_2CMe^-$ ligands, with the two halves then linked at the apical Mn sites (Mn8) *via* a combination of $\mu\text{-OMe}^-$ and $\mu\text{-}O_2CMe^-$ ligands. The oxygen atoms of the

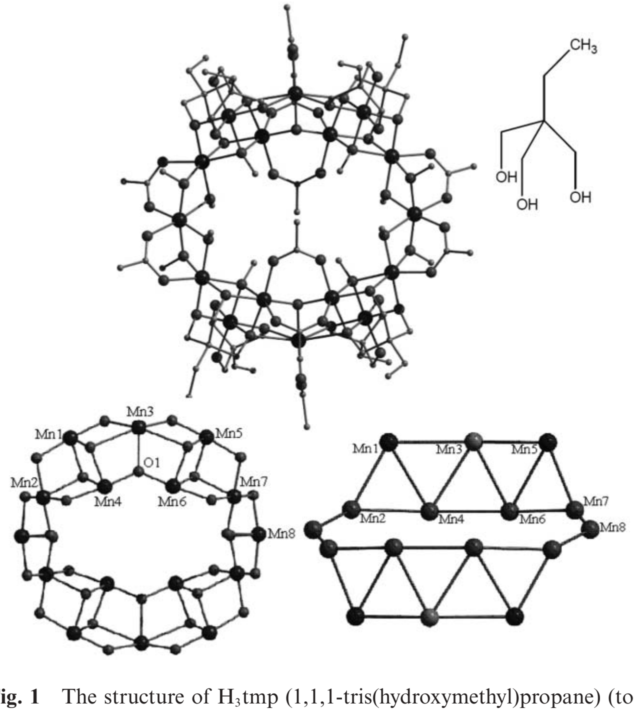

Fig. 1 The structure of H_3tmp (1,1,1-tris(hydroxymethyl)propane) (top right); the molecular structure of complex **1** (top); its metal–oxygen core and its metallic skeleton (bottom). H atoms omitted for clarity.

---

[a] *School of Chemistry, The University of Edinburgh, West Mains Road, Edinburgh, UK EH9 3JJ. E-mail: ebrechin@staffmail.ed.ac.uk; Tel: +44 (0)131-650-7545*

[b] *Department of Chemistry, University of Florida, Gainesville, Florida, 32611-7200, USA*

† The HTML version of this article has been enhanced with colour images.

‡ Electronic supplementary information (ESI) available: Magnetism data. See DOI: 10.1039/b614492f

Mn_3O_4 partial cubes are derived from η^2:η^2:η^2:μ_3-tmp^{3-} and μ_3-OMe^- ligands, and those of the Mn_3O triangles from the sole O^{2-} ions (O1 and symmetry equivalent). The Mn ions in the single-stranded central Mn_{10} wheel are all six-coordinate Mn^{III} ions in Jahn–Teller distorted octahedral geometries. The Jahn–Teller axes are not co-parallel, running both parallel and perpendicular to the plane of the wheel (Fig. SI1‡). Mn3 is a five-coordinate Mn^{II} ion in a distorted trigonal bipyramidal geometry (with two further close contacts (~2.6 Å) to oxygen arms of neighbouring μ-tmp^{3-} ligands), and Mn1 and Mn5 are six-coordinate Mn^{IV} ions in distorted octahedral geometries. These assignments were achieved on the basis of charge balance, bond length considerations and BVS analysis.[8] This therefore gives an overall formula of $[Mn^{IV}_4Mn^{III}_{10}Mn^{II}_2O_2(OMe)_{12}(tmp)_8(O_2CMe)_{10}]$. The cavity within the central Mn_{10} wheel is oval-shaped with metal–metal distances ranging from ~11 Å (Mn8–Mn8A) to ~9 Å (Mn4–Mn4A). The molecule is non-planar since the attached 'Mn_7 rods' lie above and below the plane of the central Mn^{III}_{10} wheel, and thus the overall shape of the molecule tends towards being *S-shaped* (Fig. 2). In the crystal, molecules of **1** lie in a head-to-tail fashion such that the individual *S-shaped* molecules combine to form a serpentine-like or zig-zag packing of the molecules (Fig. 2). The closest inter-molecular interactions between 'head' and 'tail' occur between terminally bound O-atoms of η^2:η^1:η^1:μ-tmp^{3-} ligands and the $–CH_2$ group (O–C, ~3.8 Å) of the equivalent tripod on the adjacent molecule. Between the serpentine-like sheets the closest contacts are between acetate oxygen atoms that effectively lie perpendicular to the central Mn_{10} wheels (O–O, >3.4 Å).

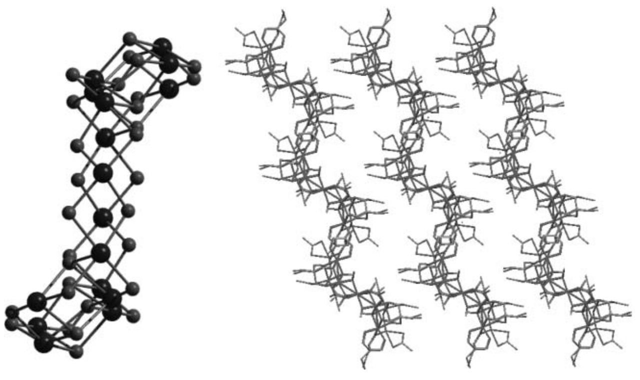

Fig. 2 The metal–oxygen core of **1** viewed parallel to the Mn_{10} plane (left); the packing of **1** in the crystal (right).

Dc susceptibility (χ_M) measurements were performed on a powdered microcrystalline sample of **1** in the ranges 5–300 K and 0.1–7 T (Fig. 3). The $\chi_M T$ value at 300 K of 47.39 cm^3 K mol^{-1} (in a 0.1 T applied field) is slightly higher than the spin-only (g = 2) value of 46.25 cm^3 K mol^{-1} expected for a complex containing two Mn^{II}, ten Mn^{III}, and four Mn^{IV} ions. The $\chi_M T$ value increases slightly with decreasing temperature to reach 51.42 cm^3 K mol^{-1} at 100 K, before increasing rapidly to reach 57.23 cm^3 K mol^{-1} at 50 K. Thereafter it increases very steeply and reaches a maximum of 88.42 cm^3 K mol^{-1} at 6.5 K, before falling slightly to a value of 87.93 cm^3 K mol^{-1} at 5 K. This suggests the complex to have a large spin ground state with the value at 5 K indicative of an $S = 14 \pm 1$ ground state. Magnetisation measurements (Fig. 3) in the range 1.8 to 10 K and between 0.5 and 0.9 T were carried out in order to determine the spin ground state value for **1**. The data were fit by a matrix-diagonalisation method using the program MAGNET to a model that assumes only the ground state is populated, includes axial zero-field splitting ($D\hat{S}_z^2$), and carries out a full powder average. The corresponding Hamiltonian is:

$$\hat{H} = D\hat{S}_z^{\,2} + g\,\mu_B\,\mu_0\hat{S}\cdot H$$

where D is the axial anisotropy, μ_B is the Bohr magneton, μ_0 is the vacuum permeability, $\hat{S}_z$ is the easy-axis spin operator, and H is the applied field. The data are plotted as reduced magnetisation $M/N\mu_B$ *versus* H/T in Fig. 3. The best fit gave $S = 14$, $g = 1.85$ and $D = -0.04$ cm^{-1}. When fields up to 7 T were employed poorer quality fits were obtained. This behaviour is characteristic of the presence of low-lying excited states. In such cases the population of excited states is difficult to avoid—even at very low temperatures. Because the fitting procedure assumes only the ground state is populated at low temperatures, the use of data collected at higher fields tends to over-estimate the value of S, and consequently the use of only low field data in the fits helps to avoid this problem, providing more reliable results. For example, for complex **1**, the value of $M/N\mu_B$ rises to approximately 36 in a field of 7 T, suggestive of $S = 18$. However this is not the true ground state, and attempts to fit the magnetization data with $S = 18$ resulted in much poorer quality fits with unreasonable parameters (D and g). The magnitude of $|D|$ is consistent with the non-parallel allignment of the Jahn–Teller axes of the Mn^{III} ions.

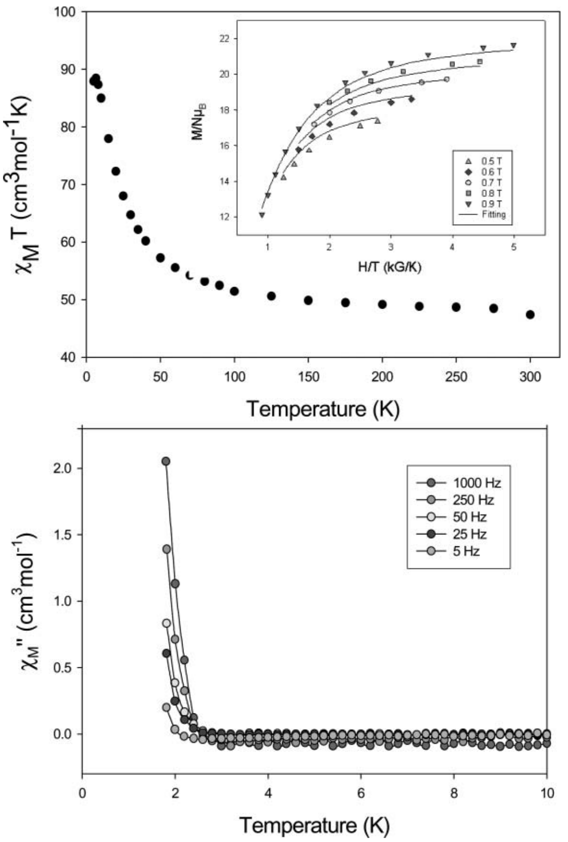

Fig. 3 Plot of $\chi_M T$ *vs.* T(top) and reduced magnetization ($M/N\mu_B$) (inset) for complex **1**. Out-of-phase (χ_M'') ac susceptibility data in the 1.8–10 K and 1000–5 Hz ranges (bottom).

To complement the dc studies, in-phase (χ_M') ac susceptibility measurements were also measured below 10 K (Fig. SI2‡). There is first an increase in the value of $\chi_M'T$ with decreasing temperature to approximately 5 K, followed by a plateau, suggesting the presence of low lying excited states with smaller S values. Such low-lying excited states are a common feature in many Mn clusters that are either of high nuclearity and thus possess a large density of spin states, or contain multiple $\mathrm{Mn^{II}}$ ions that typically promote weak exchange. Extrapolation to 0 K (from >3 K to avoid decreases due to such effects as intermolecular interactions, *etc.*) gives a value of ~94 $\mathrm{cm^3\ K\ mol^{-1}}$ for **1**, consistent with a spin ground state of $S = 14$ and $g \approx 1.9$, in agreement with the dc data. Frequency-dependent out-of-phase (χ_M'') ac susceptibility signals are seen for **1** below approximately 2.5 K (Fig. 3), but no peaks are observed. The presence of an out-of-phase signal is suggestive of single-molecule magnetism behaviour and is caused by the inability of **1** to relax quickly enough, at these temperatures, to keep up with the oscillating field.

It is difficult to speculate on the reaction pathways that lead to the formation of complex **1** (as is the case with all Mn cluster chemistry), but it has been shown previously that μ_5-bridging, fully deprotonated, tripodal alcohols favour the formation of one-dimensional rod-like complexes in Mn carboxylate chemistry.[7] Additionally the use of alcohol as solvent and the consequent presence of μ-bridging $\mathrm{MeO^-}$ ions may also favour the formation of the inner $\mathrm{Mn^{III}}_{10}$ wheel. Decametallic wheels of general formula $[\mathrm{M^{III}}_{10}(\mathrm{OR})_{20}(\mathrm{O_2CR})_{10}]$ (R = Me, Et *etc.*) are well known for $\mathrm{Fe^{III}}$, $\mathrm{Cr^{III}}$ and $\mathrm{V^{III}}$ and can be made from the reaction of the appropriate $\mathrm{M^{III}}$ triangle ($[\mathrm{M^{III}}_3\mathrm{O}(\mathrm{O_2CR})_6\mathrm{L_3}]^+$ (L = $\mathrm{H_2O}$, MeOH *etc.*) with alcohol.[5] These complexes describe a near-planar circular array of $\mathrm{M^{III}}$ ions in which each pair of metal ions is bridged by two μ-alkoxides and one μ-carboxylate. The central $[\mathrm{Mn^{III}}_{10}\mathrm{O_2}(\mathrm{OR})_{16}(\mathrm{O_2CR})_8]$ core displayed by **1** is remarkably similar (Fig. 4), perhaps suggesting that the intial step in the synthesis is the formation of a decametallic $\mathrm{Mn^{III}}$ wheel, to which further metal ions are added as a result of the presence of additional bridging (tripodal) alkoxides. This in turn suggests that the $\mathrm{Mn^{III}}$ analogue of $[\mathrm{M^{III}}_{10}(\mathrm{OR})_{20}(\mathrm{O_2CR})_{10}]$ can be made by simply reacting $[\mathrm{Mn^{III}}_3\mathrm{O}(\mathrm{O_2CR})_6\mathrm{L_3}]^+$ species with alcohol. This is currently under investigation.

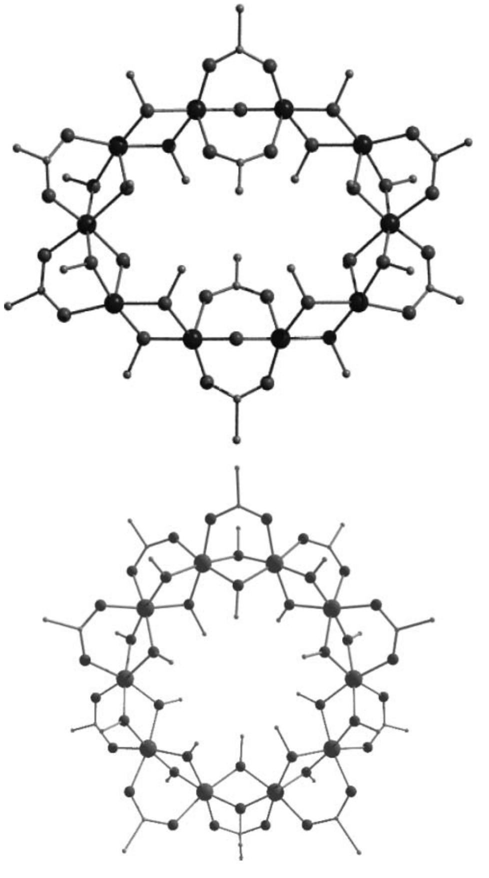

Fig. 4 The central $\mathrm{Mn^{III}}_{10}$ wheel present in **1** (top) and its comparison to the decametallic wheels of general formula $[\mathrm{M^{III}}_{10}(\mathrm{OR})_{20}(\mathrm{O_2CR})_{10}]$ (bottom).

In conclusion we have synthesised a rare example of a high-spin, high nuclearity Mn wheel—indeed the $S = 14$ ground state displayed by **1** is the largest seen for any Mn wheel-like structure. Single crystal hysteresis loop and relaxation measurements performed on **1** using micro-SQUID apparatus will be reported in a full paper.

Notes and references

§ Diffraction data for **1** were collected at 150 K on a Bruker Smart Apex CCD diffractometer equipped with an Oxford Cryosystems LT device. The structure was solved by direct methods (SHELXS) and refined by full-matrix least squares against F^2 (CRYSTALS). Hydrogen atoms were positioned geometrically and refined using the riding model. The asymmetric unit is a 'half wheel', with the other half being generated by a crystallographic centre of symmetry. $\mathrm{C_{80}H_{154}Mn_{16}O_{58}}$, $M = 3145.42$, triclinic $P\bar{1}$, $a = 13.4140(4)$, $b = 15.9060(4)$, $c = 17.9870(5)$ (Å), $\alpha = 66.487(2)$, $\beta = 82.684(2)$, $\gamma = 71.820(2)°$, $V = 3343.42(17)$ (Å^3), $Z = 1$, $T = 150(2)$ K, data/restraints/parameters = 15311/408/691, $R1 = 0.0457$ [9419 data], $wR2 = 0.1436$. CCDC reference number 623039. For crystallographic data in CIF or other electronic format see DOI: 10.1039/b614492f (Anal. Calcd for $\mathrm{Mn_{16}C_{80}H_{154}O_{58}}$: C, 32.87; H, 5.31. Found: C, 32.44; H, 5.00%.)

1 (*a*) R. Sessoli, H. L. Tsai, A. R. Schake, S. Y. Wang, J. B. Vincent, K. Folting, D. Gatteschi, G. Christou and D. N. Hendrickson, *J. Am. Chem. Soc.*, 1993, **115**, 1804; (*b*) R. Sessoli, D. Gatteschi, A. Caneschi and M. A. Novak, *Nature*, 1993, **365**, 141; (*c*) D. Gatteschi and R. Sessoli, *Angew. Chem., Int. Ed.*, 2003, **42**, 268; (*d*) A. Caneschi, D. Gatteschi, R. Sessoli, A. L. Barra, L. C. Brunnel and M. Guillot, *J. Am. Chem. Soc.*, 1991, **113**, 5873.

2 G. Aromí and E. K. Brechin, *Struct. Bonding*, 2006, **122**, 1.

3 D. N. Hendrickson, G. Christou, H. Ishimoto, J. Yoo, E. K. Brechin, A. Yamaguchi, E. M. Rumberger, S. M. J. Aubin, Z. Sun and G. Aromí, *Mol. Cryst. Liq. Cryst.*, 2002, **376**, 301.

4 A. J. Tasiopoulos, A. Vinslava, W. Wernsdorfer, K. A. Abboud and G. Christou, *Angew. Chem., Int. Ed.*, 2004, **43**, 2117.

5 (*a*) E. J. L. McInnes, S. Piligkos, G. A. Timco and R. E. P. Winpenny, *Coord. Chem. Rev.*, 2005, **249**, 2577; (*b*) R. Laye, M. Murrie, S. Ochsenbein, A. R. Bell, S. J. Teat, J. Raftery, H.-U. Güdel and E. J. L. McInnes, *Chem.–Eur. J.*, 2003, **9**, 6215; (*c*) K. L. Taft, C. D. Delfs, G. C. Papaefthymiou, S. Foner, D. Gatteschi and S. J. Lippard, *J. Am. Chem. Soc.*, 1994, **116**, 823; (*d*) H. Kumagai and S. Kitagawa, *Chem. Lett.*, 1996, 471.

6 (*a*) M. Murugesu, W. Wernsdorfer, K. A. Abboud and G. Christou, *Angew. Chem., Int. Ed.*, 2005, **44**, 892; (*b*) S.-X. Liu, S. Lin, B.-Z. Lin, C.-C. Lin and J. Q. Huang, *Angew. Chem., Int. Ed.*, 2001, **40**, 1084; (*c*) D. Foguet-Albiol, T. A. O'Brien, W. Wernsdorfer, B. Moulton, M. J. Zaworotko, K. A. Abboud and G. Christou, *Angew. Chem.*, 2005, **44**, 897; (*d*) E. M. Rumberger, S. J. Shah, C. C. Beedle, L. N. Zakharov, A. L. Rheingold and D. N. Hedrickson, *Inorg. Chem.*, 2005, **44**, 2742.

7 (*a*) E. K. Brechin, *Chem. Commun.*, 2005, 5141; (*b*) G. Rajaraman, M. Murugesu, M. Soler, W. Wernsdorfer, M. Helliwell, S. J. Teat, G. Christou and E. K. Brechin, *J. Am. Chem. Soc.*, 2004, **126**, 15445.

8 H. H. Thorp, *Inorg. Chem.*, 1992, **31**, 1585.